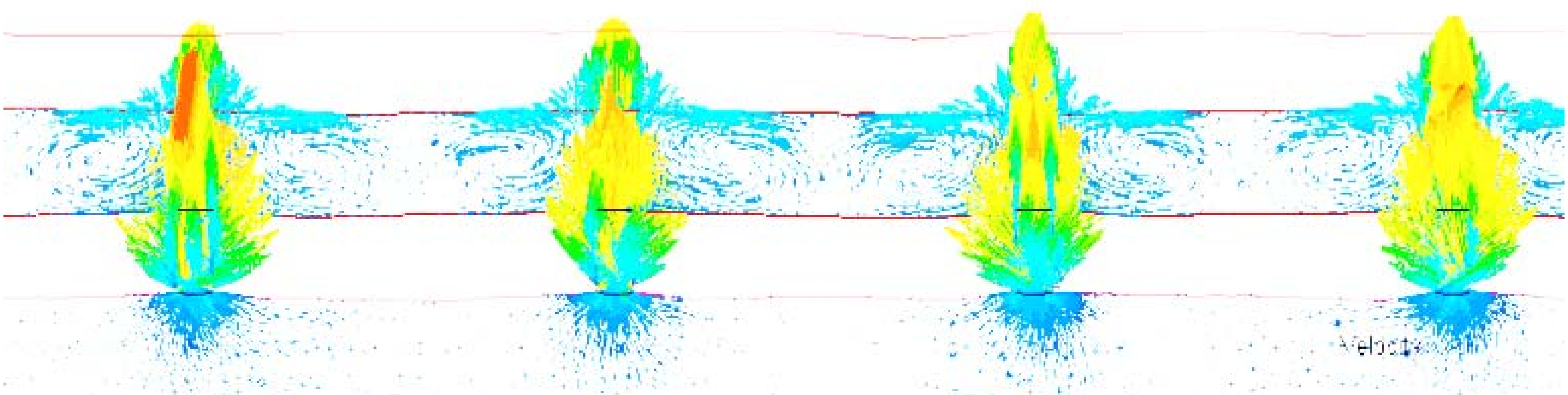

Research on PFC Heat and Mass Transfer

Presented by Neil Morley, on behalf of:

A. Ying, F. C. Li, A. Kohli, H. Liu, M. A. Abdou

PFC Meeting
June 20-22, 2012
PPPL, Princeton, NJ

Outline

- PFC Heat and Mass Transfer Simulation
  - Tritium retention and permeation in FW/Divertor
  - Helium cooling for high heat flux removal
  - Thermomechanics for FW/Divertor components
- Synergistic Blanket Research
  - Liquid metal MHD, heat and tritium transport
    - E.g. High temperature liquid metal loop for channel flow
    - Small scale free surface and wetting experiments
  - Ceramic breeder and Be thermomechanics and tritium transport

The goal of modeling is to build an integrated multi-physics simulation predictive capability

- Integral physics approach (multi-physics)
- Representative component geometry (instead of 1-D or surface only)
- Coupled advanced simulation (e.g. DEM + FEM for thermomechanics, MD and Finite volume for modeling tritium transport due to surface damage

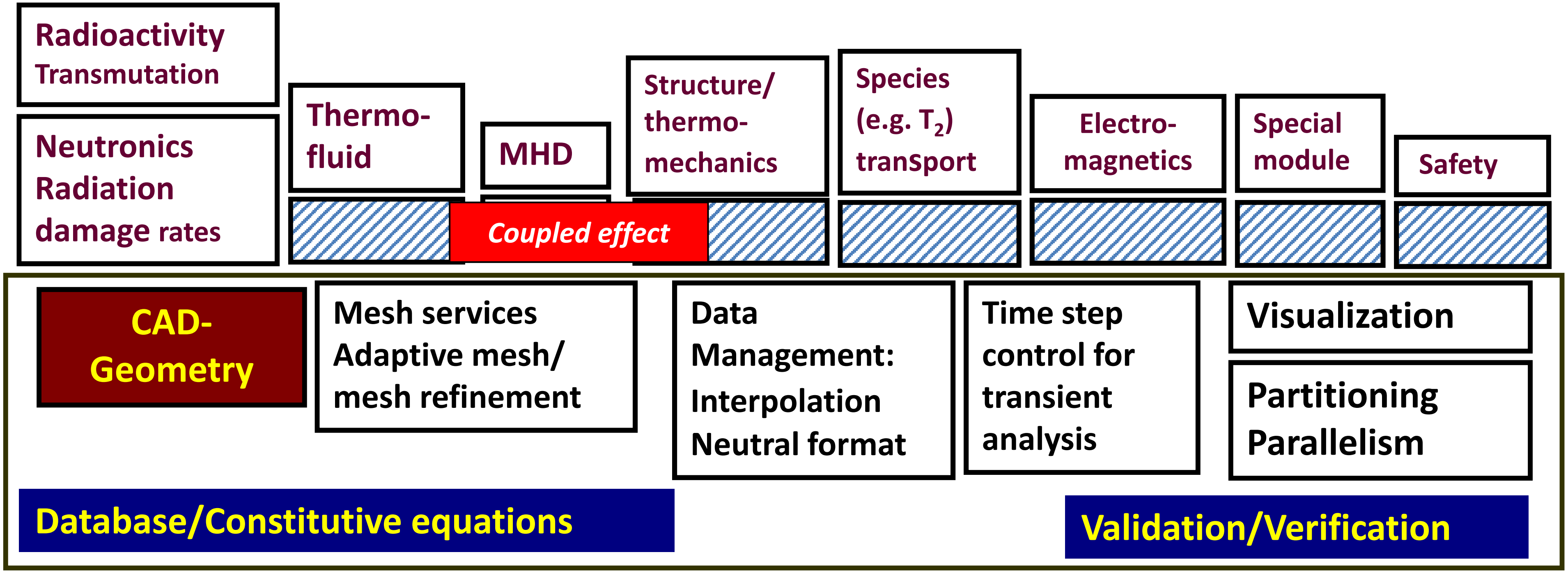

Radioactivity
Transmutation

Neutronics
Radiation
damage rates

Thermo-fluid

MHD

Structure/ thermo-mechanics

Species (e.g. T_2) transport

Electro-magnetics

Special module

Safety

Coupled effect

CAD-Geometry

Mesh services
Adaptive mesh/ mesh refinement

Data Management:
Interpolation
Neutral format

Time step control for transient analysis

Visualization

Partitioning
Parallelism

Database/Constitutive equations

Validation/Verification

1. Tritium concentration profiles throughout the whole FW and coolant

Modeling tools previously developed in the US : TMAP-7 (Oct. 2004), DIFFUSE

☐ Initial Focused on materials: Tungsten, Beryllium

☐ Mechanisms (all temperature dependent):

- Implantation (implantation range, Gaussian profile with mean range and standard deviation) and reflection
- Recombination (enhanced by surface damage as seen in Be)
- Erosion and dust (tritium returns to plasma through eroded Be/Tungsten)
- Diffusion / Permeation / Thermodiffusion (Soret)
- Trap and De-trap due to ion induced defects, and ion induced defect production (following Gaussian implantation profile)
- Trap and De-trap due to intrinsic defects
- Trap and De-trap due to neutron damage (trap energy), correlation between dpa and trap site
- Flux conservation at the material interfaces and solubility
- Surface topology (surface alters due to re-deposition)

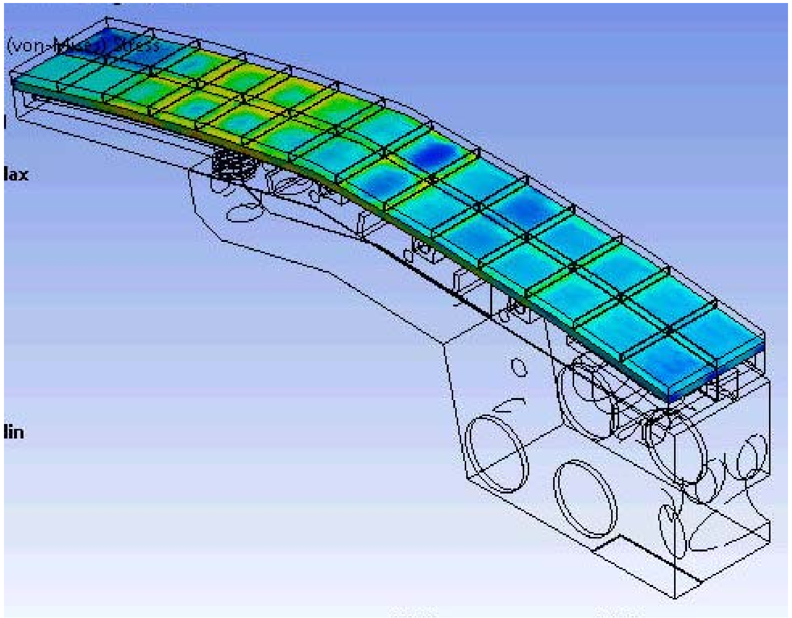

☐ Progress is being made by comparison with the available data

Tritium Retention and Permeation in FW/Divertor

Initially: COMSOL is used as a benchmark code to properly model the underlying physics

Later models have to be implemented in a CFD-like code in order to handle larger components

A. Tungsten wall: Uncertainty in recombination coefficient

High incident flux: $1.2\times10^{22}\ m^{-2}s^{-1}$

Example Implantation range -5.6 nm (200ev) Gaussian profile

Impact of uncertainty of Kr is small at high flux

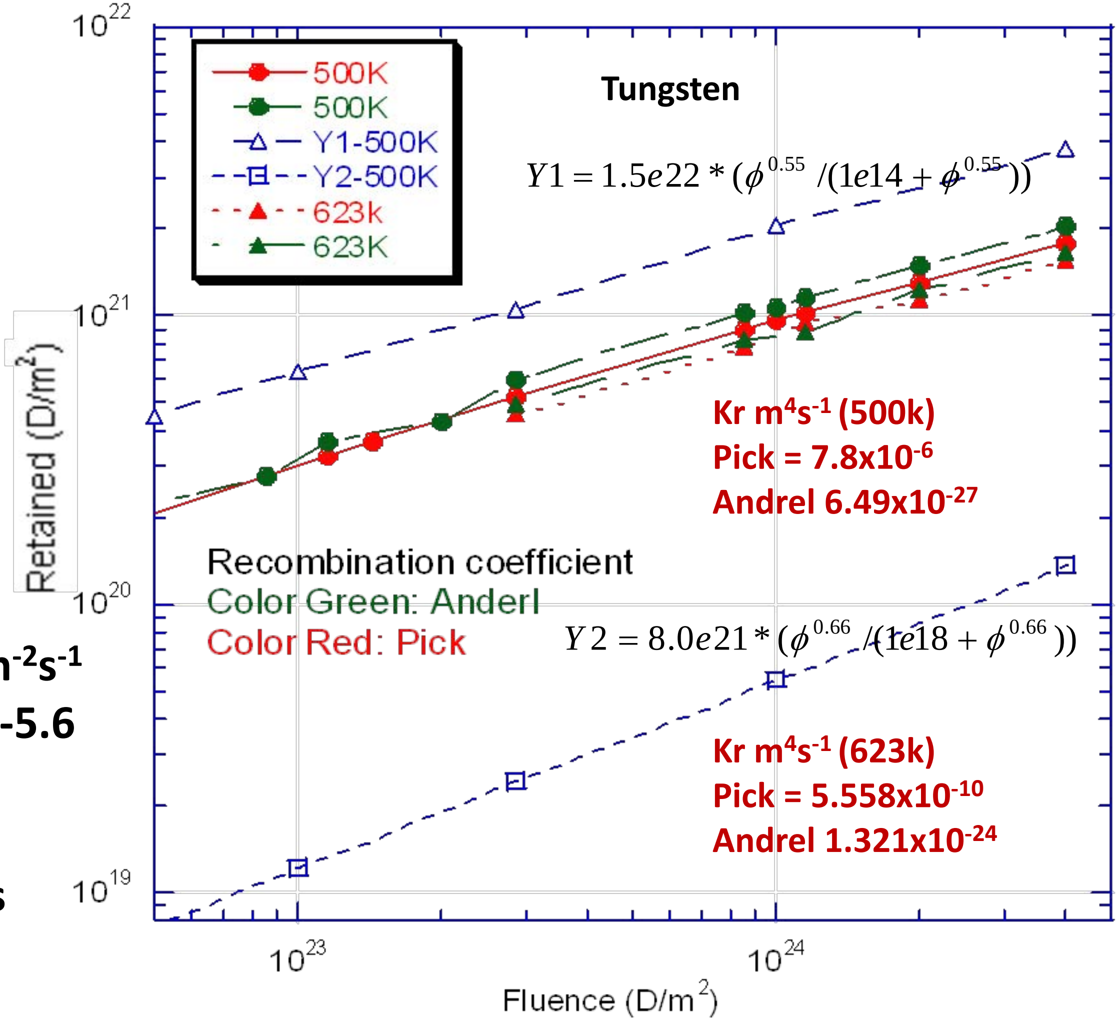

Tungsten

$Y1 = 1.5e22 * (\phi^{0.55} / (1e14 + \phi^{0.55}))$

$Y2 = 8.0e21 * (\phi^{0.66} / (1e18 + \phi^{0.66}))$

Recombination coefficient

Color Green: Anderl

Color Red: Pick

Kr m^4s^{-1} (500k)
Pick = 7.8×10^{-6}
Andrel 6.49×10^{-27}

Kr m^4s^{-1} (623k)
Pick = 5.558×10^{-10}
Andrel 1.321×10^{-24}

Tungsten wall Tritium Retention and Permeation (Cont'd)

The increase of the ion-induced trap density is modeled by (Ogorodnikova, Roth, and Mayer (2008):

$$dW/dt = (1-r)I_o\varphi(x)(1-\eta W/W_m)$$

Deuterium implantation profile

η : The rate of defect creation
W_m : the maximum defect concentration

At a lower incident flux of $3\text{x}10^{19}$ $m^{-2}s^{-1}$, the difference in recombination coefficient can be reflected in concentration profile as well as the retained quantity.

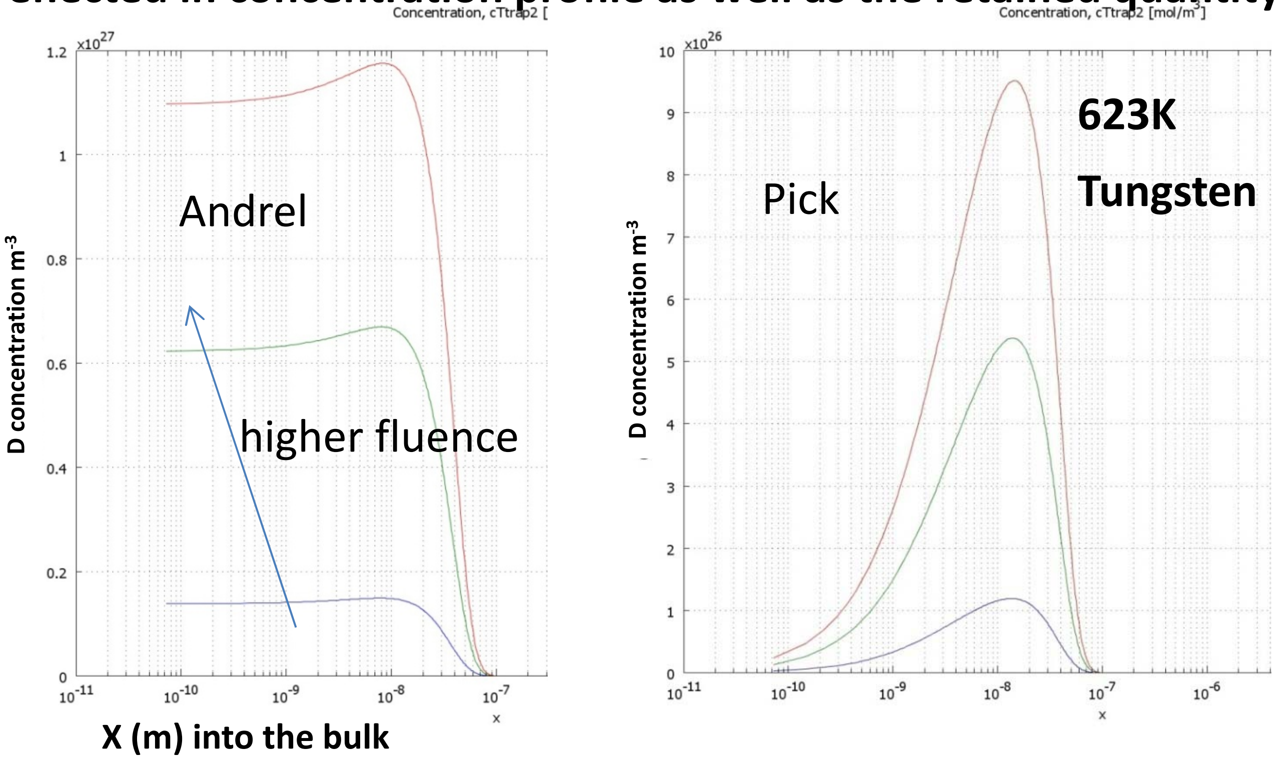

D retained in Ion-induced traps

Be wall: Deuterium/tritium retention dominating underlying physics- erosion, migration, (codeposition)

Deuterium/tritium removal from Be PFC must be included in the modeling to account for the lower retention found in experiments. In literature, this is modeled by:

$$J_r = -(2K_r n_o^2 + u n_o)$$

Mobile atom concentration at the surface

u: erosion face velocity

$$K_r' = 3.4e-29 * \exp\left(\frac{-0.28ev}{kT}\right) * \left[1 + \exp\left(\frac{10 n_o}{n_{sat}} - 10\right)\right] + \frac{u}{1+n_o}$$

Allowing enhanced recombination as the surface concentration reaches the saturation level

Saturation value of the hydrogen atom concentration in Be

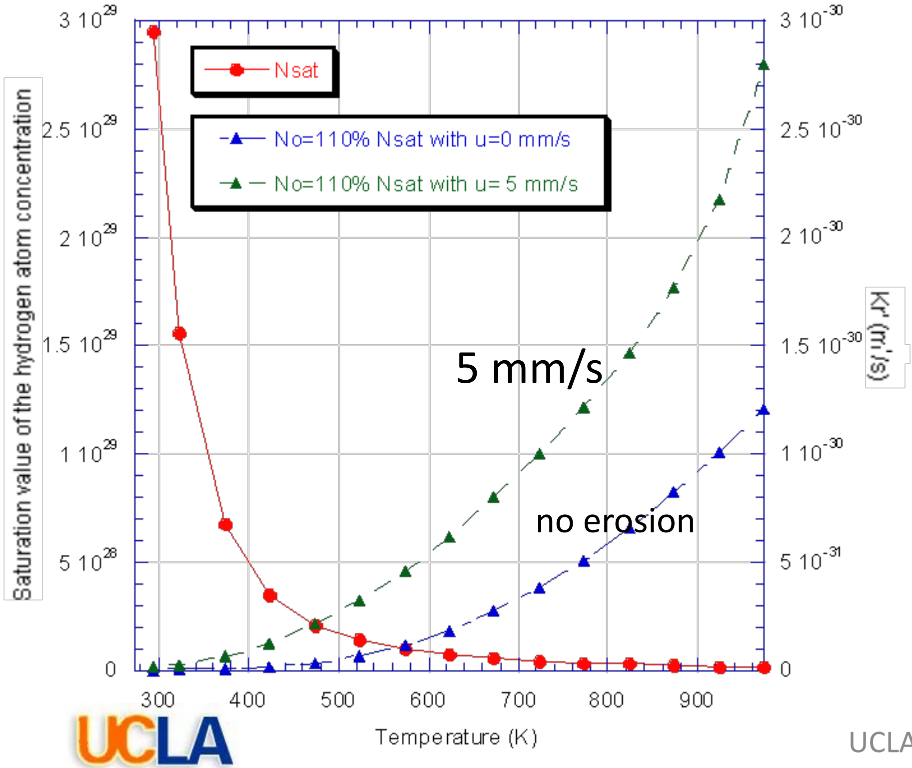

At small u, deuterium/tritium removed by erosion is already significantly more than the recombination enhanced by saturation effect.

Incorporation of erosion effect allows reproducing experimental data

Role of diffusivity: A higher diffusivity leads to a lower tritium retention

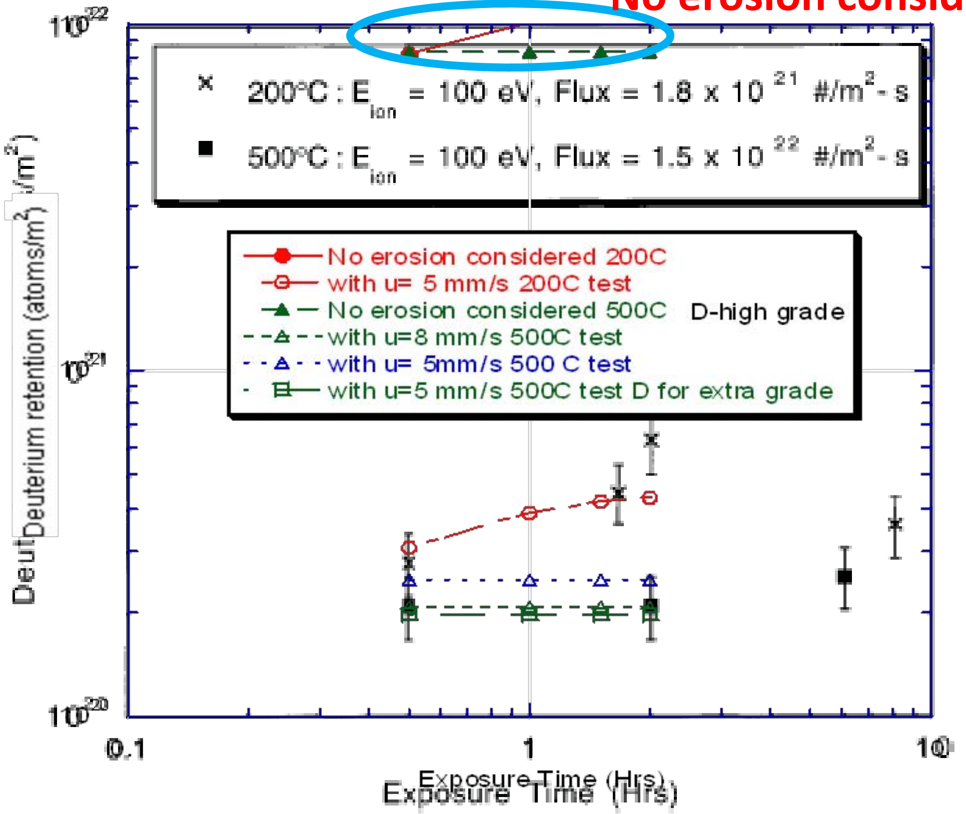

Abramov et al. (1990)

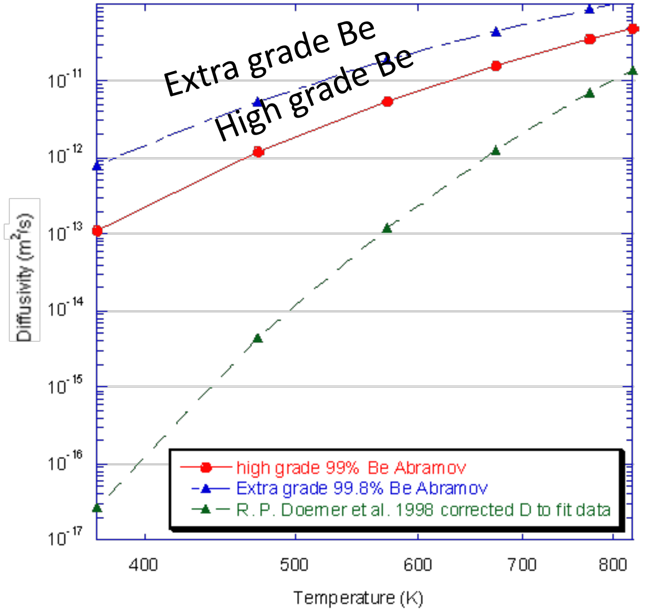

Deuterium diffusivity as a function of temperature

Fig. 4. Deuterium retention in beryllium exhibits only a weak dependence on increasing fluence.

Fig. 4. taken from R. P. Doerner et al./Journal of Nuclear Materials 257 (1998) p.55

Both tritium retention and permeation into coolant from ion flux appear low after 1001 cycles.

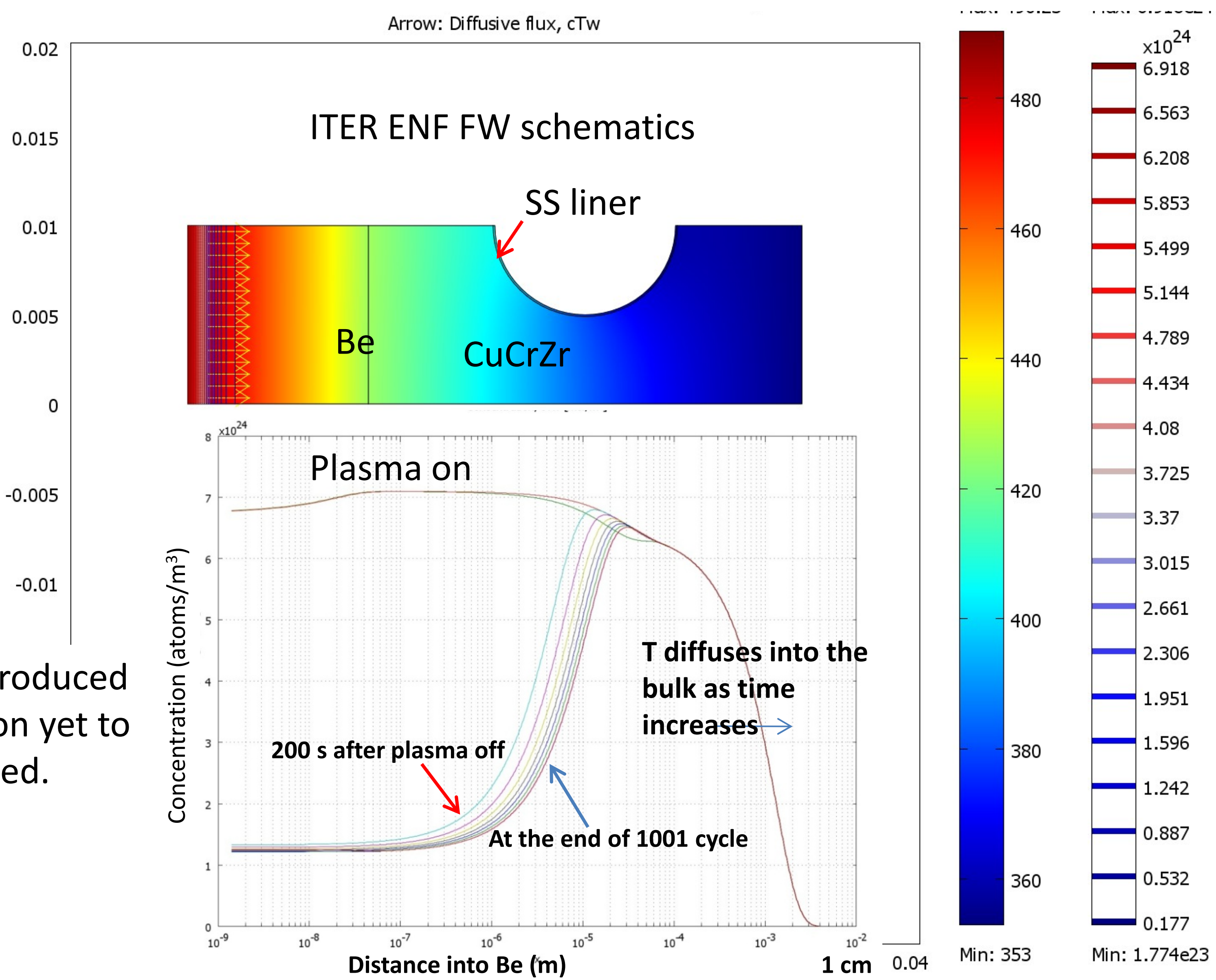

Tritium produced by neutron yet to be included.

2. Helium impinging jet cooling for high heat flux FW and Divertor

GOAL

- Study the effect of jet interactions to optimize heat transfer and pressure drop
- Access validity of various turbulence models
- Train new student in gas cooling simulations

CONSTRAINTS

- Ferritic steel temperature < 550 ^{0}C
- velocity < compressible limit (~ 500 m/s)
- Constant flow rate when increasing jet #

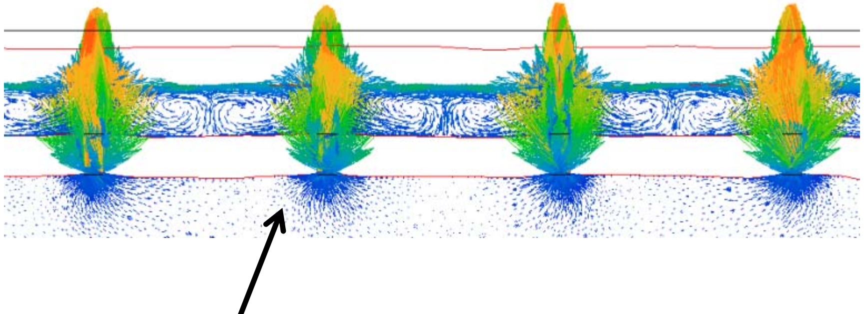

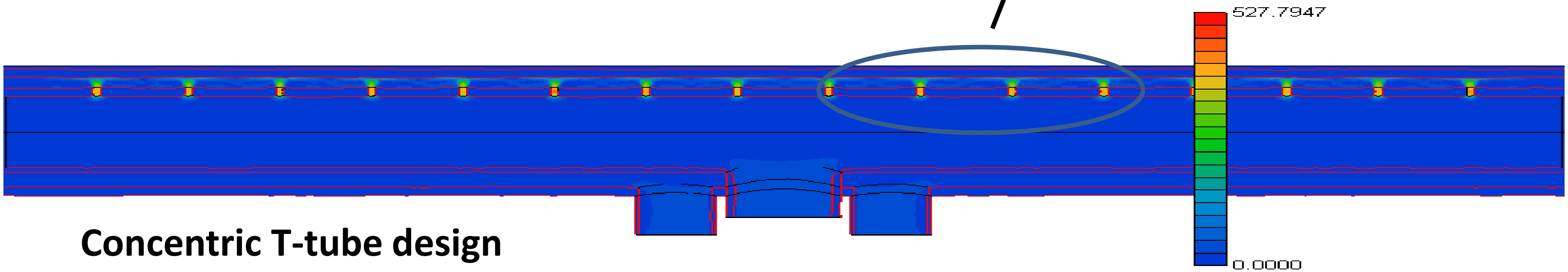

Concentric T-tube design

Comparison between simulations using MPAKN k-ε and SST k-ω models in SC/Tetra

Flow rates for the following simulations were kept constant and corresponded to a 250 K increase in He inlet temperature . All jets have the same diameter.

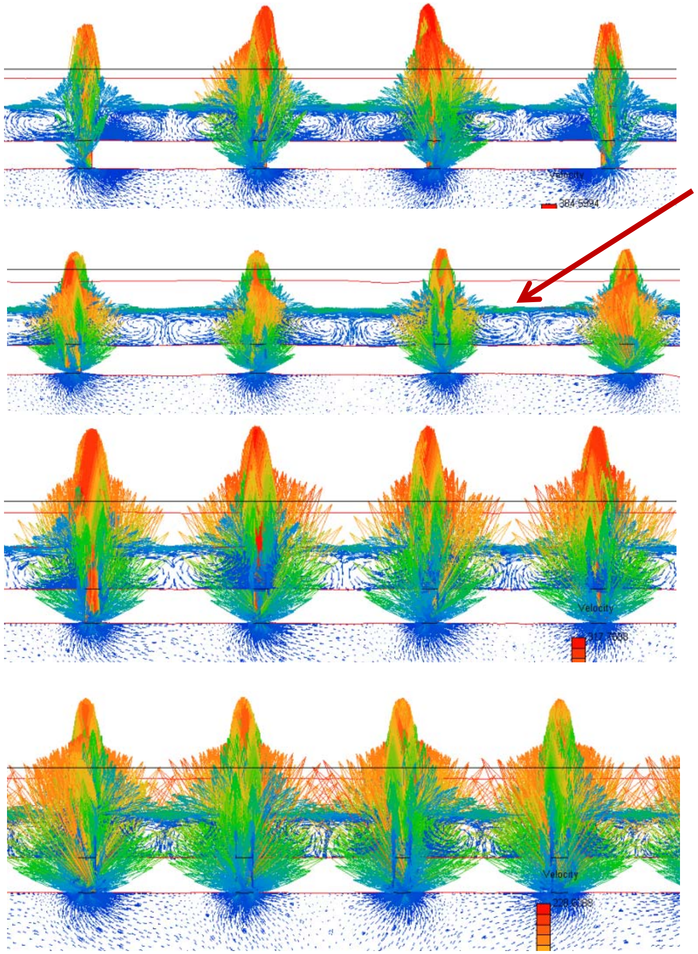

Results from 14, 16, 18, 20 jet configurations with SST **k-ω** model

- Jet-to-jet interaction more pronounced with increasing number of jets, especially in the k-ω model
- Velocity predictions from both models agree fairly well with each other (<5 % for most cases) and were below the compressible limit

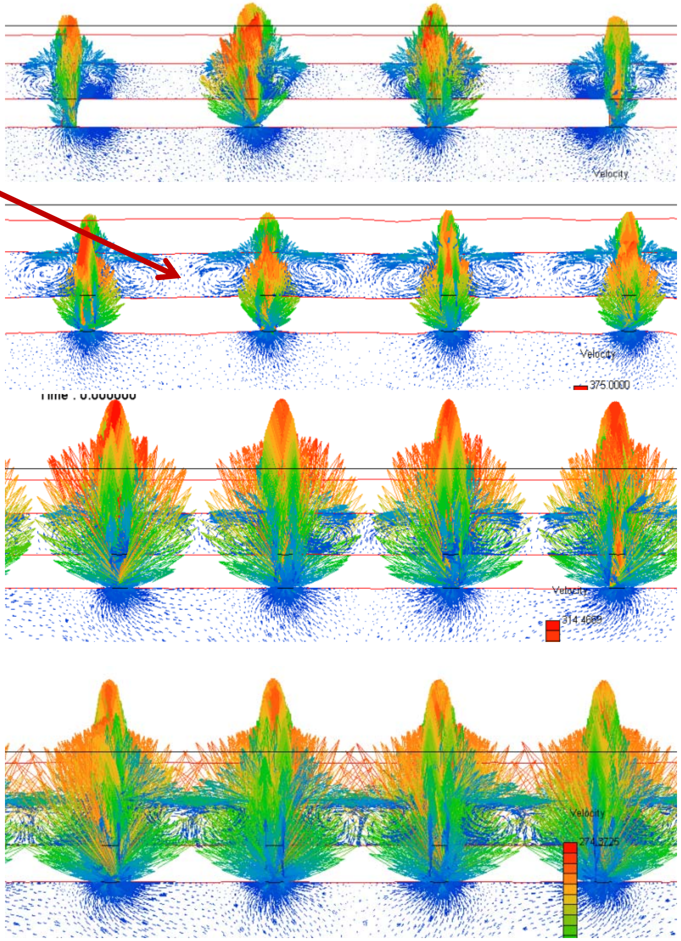

Results from 14, 16, 18, 20 jet configurations with MPAKN **k-ε** model

3. Thermomechanics of FW/Divertor Components: Impact of Be tile size on finger stresses at CuCrZr heat sink for ITER

An EHF ITER FW is composed of ~40 pairs of twin fingers. In PDR design, they are structurally locked to arm and beam through pins/lugs. Each has hypervaportron CuCrZr heat sink. They are designed to remove a local, peak heat flux up to 4.7 MW/m^2.

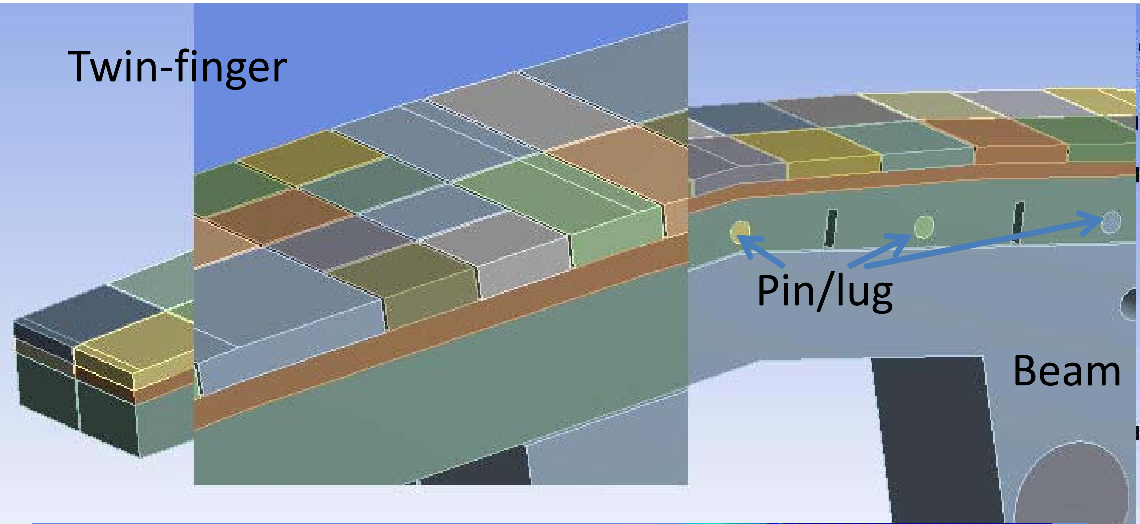

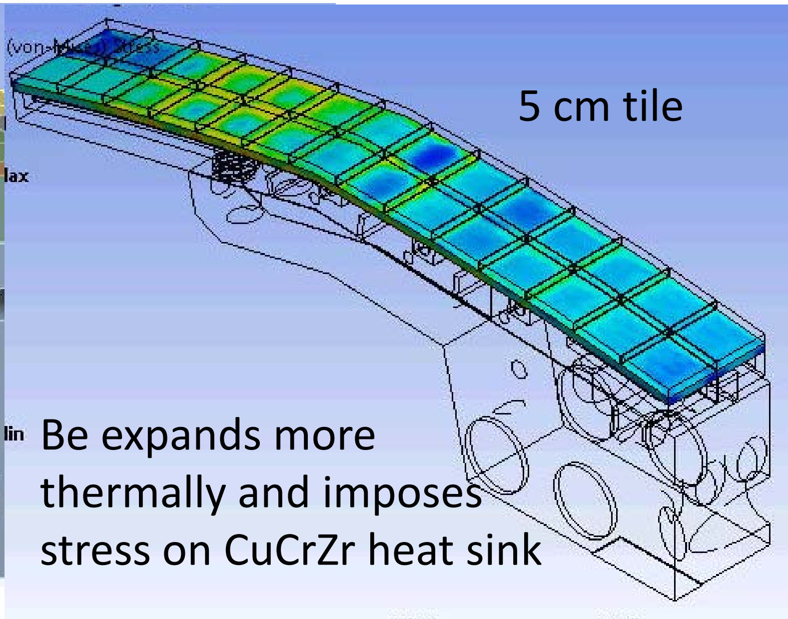

Be expands more thermally and imposes stress on CuCrZr heat sink

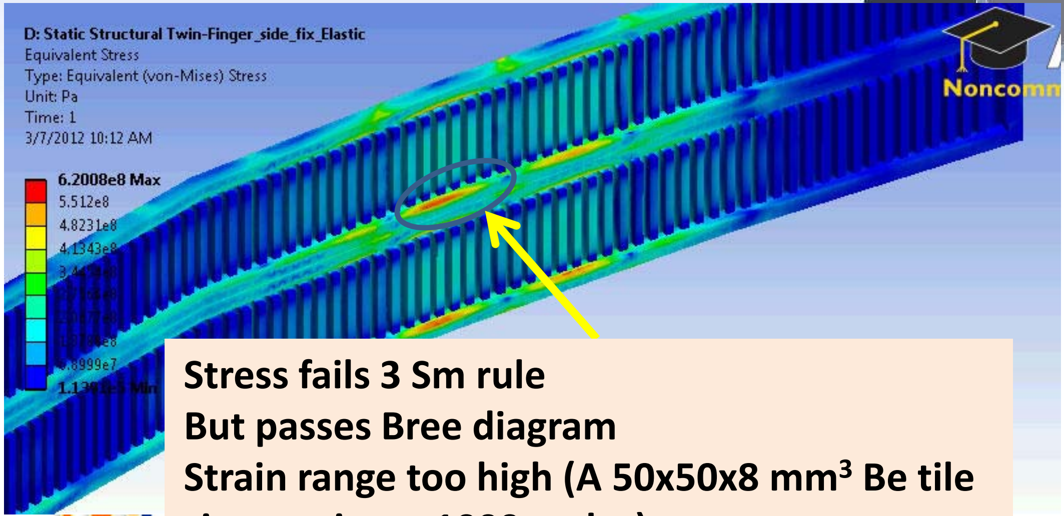

D: Static Structural Twin-Finger_side_fix_Elastic
Equivalent Stress
Type: Equivalent (von-Mises) Stress
Unit: Pa
Time: 1
3/7/2012 10:12 AM

Stress fails 3 Sm rule
But passes Bree diagram
Strain range too high (A 50x50x8 mm^3 Be tile size survives <1000 cycles)

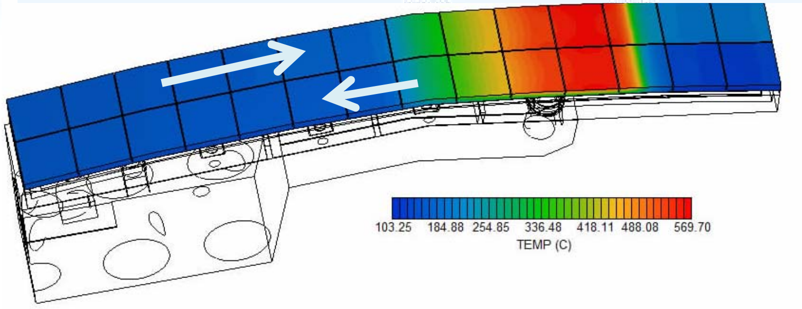

Be surface temperature (max temp ~ 570 C) Maximum surface heat load for the case shown = 3.8 MW/m2)

Elastic Analysis -Be Tile 25x 25 x (6+2) mm^3

Calculated IC (ITER Criteria)3323 **equivalent strain range for a selected path** from **elastic analysis** give values of ~0.36% and about 5400 numbers of cyclic operations allowable (Where Strain range = elastic strain range ($\Delta\varepsilon_1$) + corrections for effects of plasticity ($\Delta\varepsilon_2$+ $\Delta\varepsilon_3$ + $\Delta\varepsilon_4$))

Fatigue	
Nd	~5400
Temperature T degC	253.3
Δε(%)	0.35951586
$\Delta\varepsilon= \Delta\varepsilon_1+\Delta\varepsilon_2+\Delta\varepsilon_3+\Delta\varepsilon_4$	0.003595159
Δε1	0.002735466
Δσ_tot (P_tot#1)	360.94
Δε2	5.20712E-05
Δε_cyclic	0.000209605
Δε_t(%)	0.020960483
Δσ	17.3287
ΔP_eff	17.3287
Pm	11.56
Pb+PL	20.17
$\Delta\varepsilon3 =(K\varepsilon-1)(\Delta\varepsilon_1+\Delta\varepsilon_2)$	-0.000696884
Kε	0.75
$\Delta\varepsilon4= (Kv-1)\Delta\varepsilon_1$	0.001504506
Kv	1.55
$\Delta\varepsilon=[(K_\varepsilon+K_v-1)*(\Delta\varepsilon_1+\Delta\varepsilon_2)]$	0.003623798

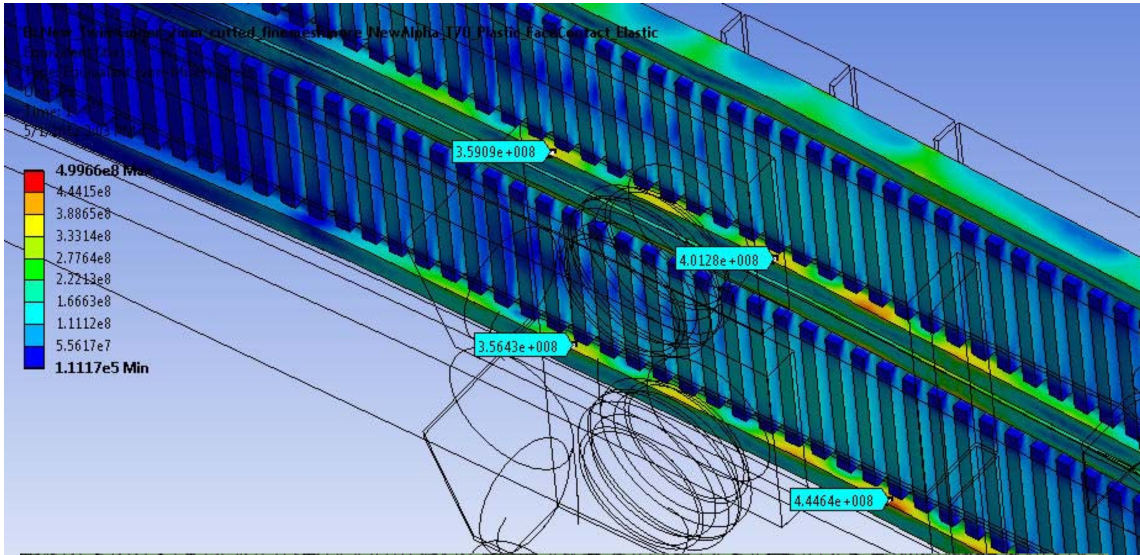

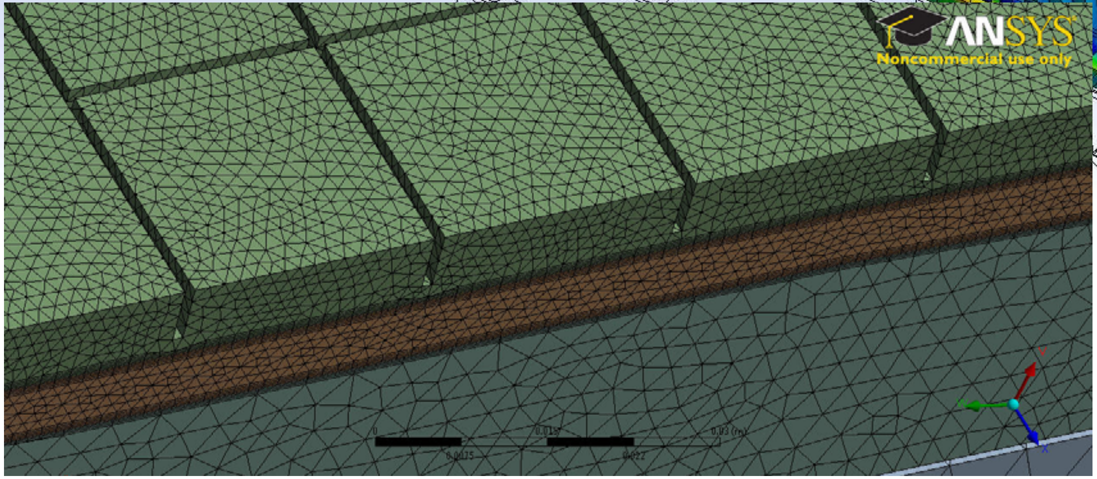

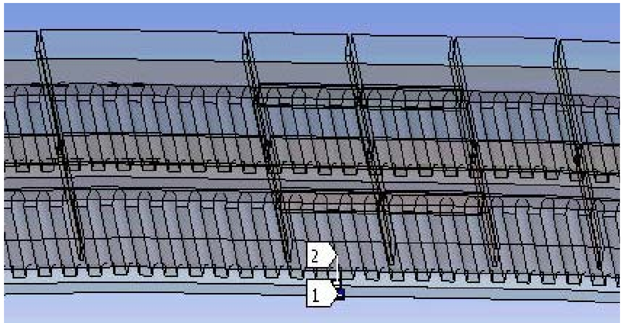

Transient elasto-plastic analysis was performed over 5 ITER Induction cycles, which revealed time dependent component strain tensor behavior

The equivalent scalar strain range between the states t and t’ is calculated using the difference between the strain tensor components at the states t and t’:

$$\varepsilon_{xx}(t,t') = \varepsilon_{xx}(t) - \varepsilon_{xx}(t')$$

$$\overline{\varepsilon(t,t')} = \frac{\sqrt{2}}{3}\left\{\left[\varepsilon_{xx}(t,t') - \varepsilon_{yy}(t,t')\right]^2 + \left[\varepsilon_{yy}(t,t') - \varepsilon_{zz}(t,t')\right]^2 + \left[\varepsilon_{zz}(t,t') - \varepsilon_{xx}(t,t')\right]^2 + 6\left[\varepsilon_{xy}^2(t,t') + \varepsilon_{yz}^2(t,t') + \varepsilon_{zx}^2(t,t')\right]\right\}^{1/2}$$

Transient Results (SDC-IC B 2630)

	t5400	t5800					**delta_Pstrain**	
εp_{xx}	6.39E-04	1.76E-03		$\varepsilon p_{xx}(t,t')$	1.12E-03		**1.51E-03**	
εp_{yy}	-7.84E-05	-3.29E-04		$\varepsilon p_{yy}(t,t')$	-2.50E-04			
εp_{zz}	-5.60E-04	-1.43E-03		$\varepsilon p_{zz}(t,t')$	-8.69E-04			
εp_{xy}	-5.34E-05	6.93E-04		$\varepsilon p_{xy}(t,t')$	7.46E-04			
εp_{yz}	5.21E-05	-6.25E-05		$\varepsilon p_{yz}(t,t')$	-1.15E-04			
εp_{zx}	2.18E-04	-1.04E-04		$\varepsilon p_{zx}(t,t')$	-3.22E-04			
	t5400	t5800					**delta_Estrain**	
ε_{xx}	-7.47E-04	1.11E-03		$\varepsilon_{xx}(t,t')$	1.86E-03		**2.09E-03**	
ε_{yy}	5.99E-05	-1.79E-05		$\varepsilon_{yy}(t,t')$	-7.78E-05			
ε_{zz}	2.51E-04	-5.21E-04		$\varepsilon_{zz}(t,t')$	-7.72E-04			
ε_{xy}	-5.55E-04	4.97E-04		$\varepsilon_{xy}(t,t')$	1.05E-03			
ε_{yz}	6.43E-05	-8.93E-05		$\varepsilon_{yz}(t,t')$	-1.54E-04			
ε_{zx}	2.88E-04	-2.37E-04		$\varepsilon_{zx}(t,t')$	-5.25E-04			
							Total Strain Range	
Elastic strain							**3.59E-03**	
	1.07E-03	1.32E-03						
		2.52E-04						

Similar to the elastic analysis result

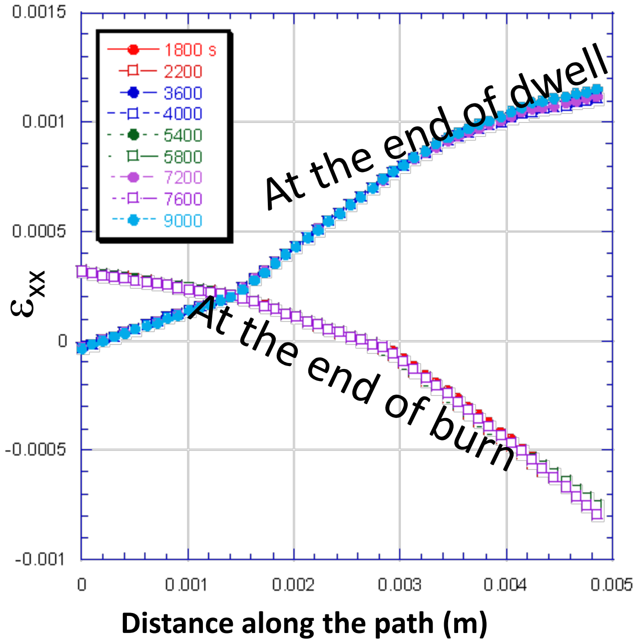

X component elastic strain tensor as a function of time shows expansion and shrinkage behavior

Reducing Be tile size to 12x12x (6+2) seems not reducing the stress enough in some region with a 4.7 MWm^{-2} profile

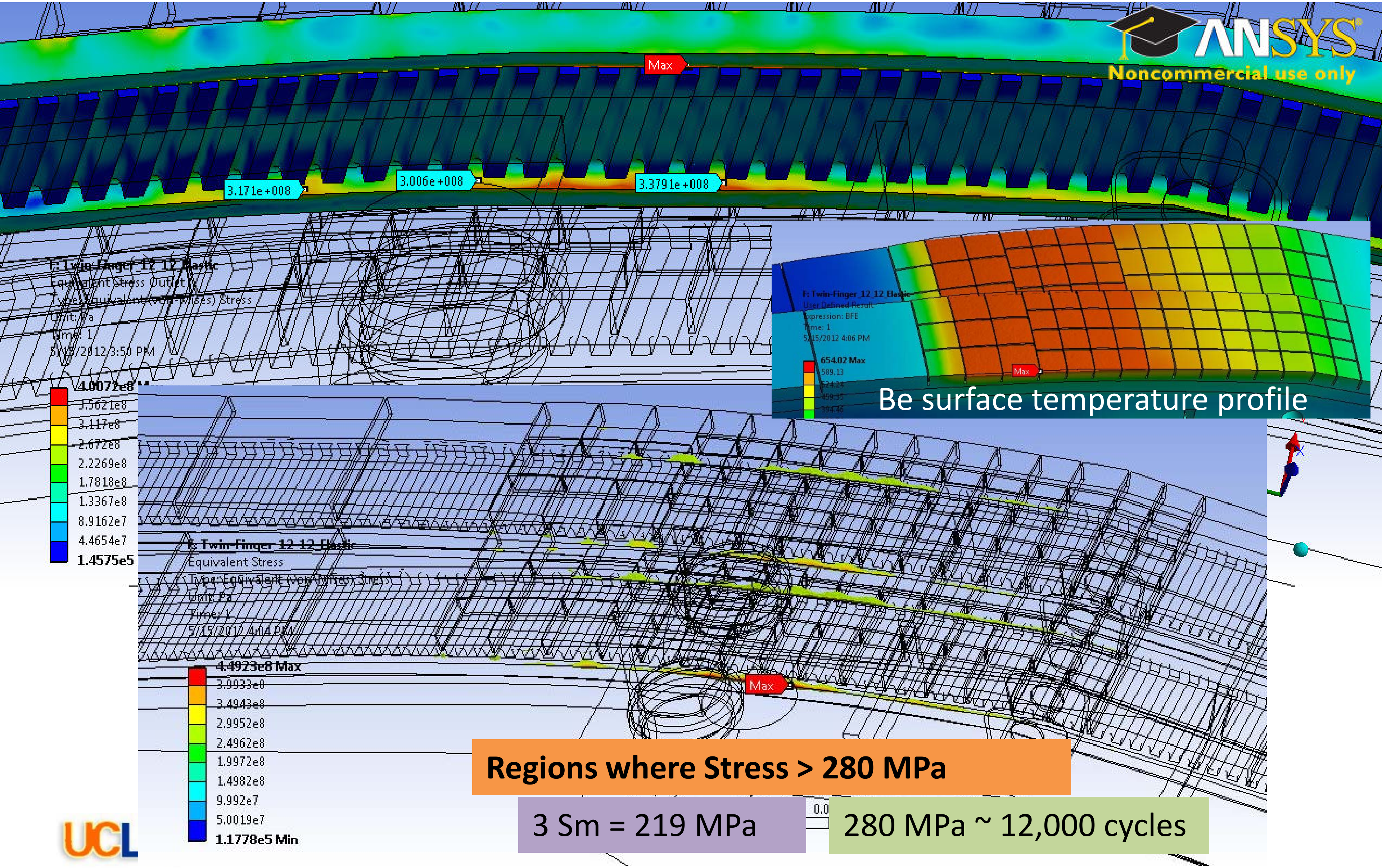

Be surface temperature profile

Regions where Stress > 280 MPa

3 Sm = 219 MPa

280 MPa ~ 12,000 cycles

Post PDR box-like finger design (less structurally constrained- no pin/lug)

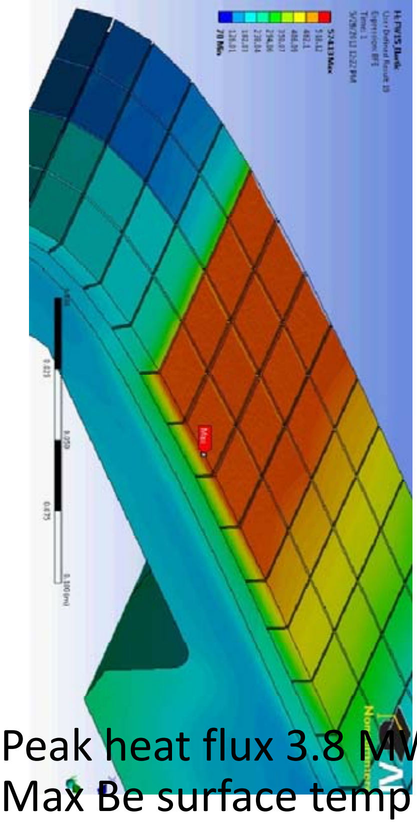

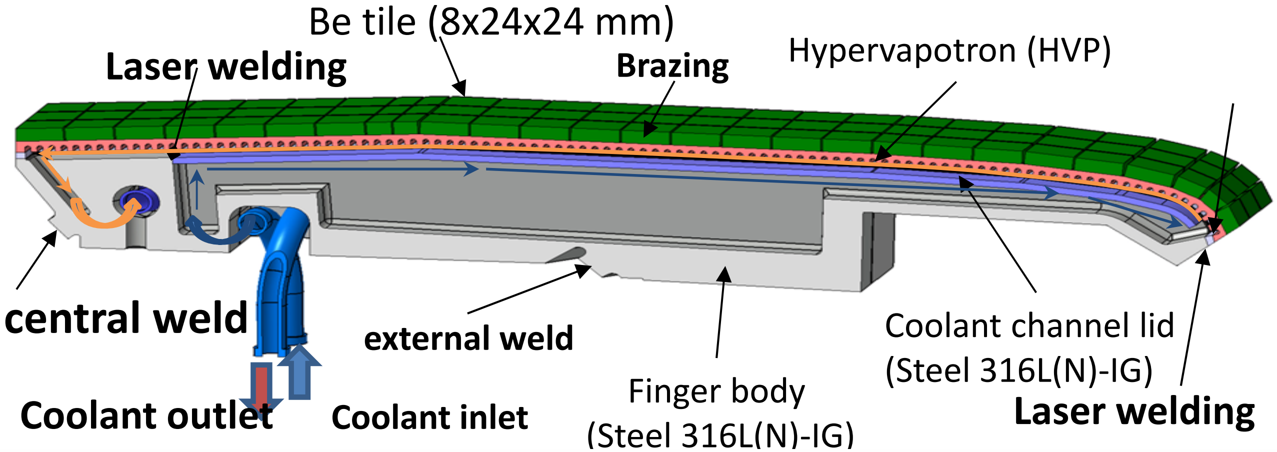

Be tile (8x24x24 mm)

Laser welding

Brazing

Hypervapotron (HVP)

central weld

external weld

Coolant channel lid (Steel 316L(N)-IG)

Finger body (Steel 316L(N)-IG)

Coolant outlet

Coolant inlet

Laser welding

Peak heat flux 3.8 MW/m^2
Max Be surface temp = 574C
Water velocity = 2m/s

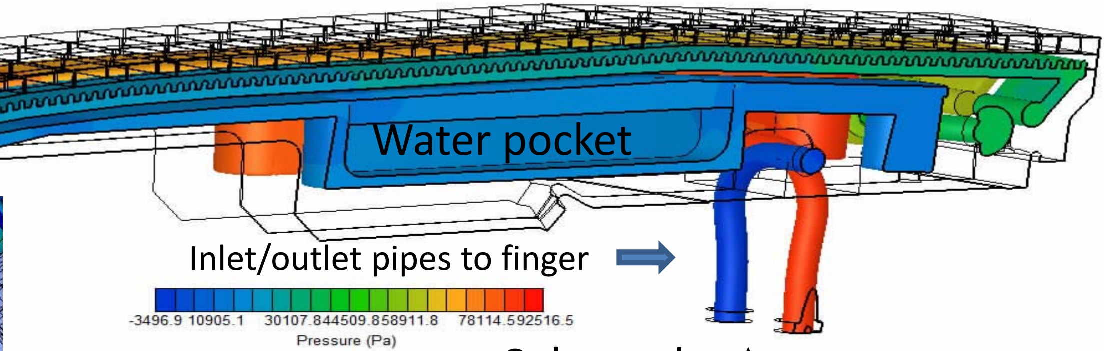

Color code: Δ pressure

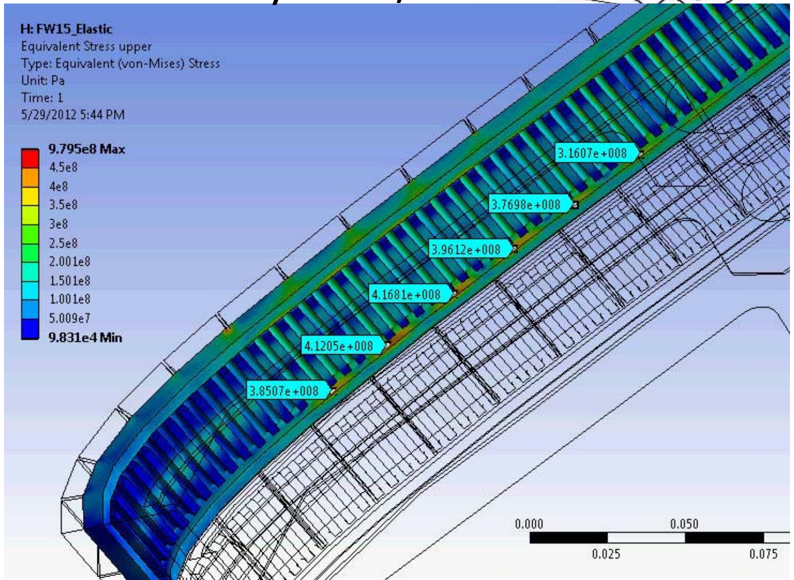

H: FW15_Elastic
Equivalent Stress upper
Type: Equivalent (von-Mises) Stress
Unit: Pa
Time: 1
5/29/2012 5:44 PM

- Tile size: 24x24x 8 mm^3
- Similar high von Mises stress found in the CuCrZr heat sink side wall
- Smaller tiles are needed

Summary/Future work

- Heat and Mass Transfer PFC Activities
  - Tritium retention and permeation in FW/Divertor
    - Be/W sphere experiments and TMAP as benchmark
    - More complex geometries
  - Helium cooling for high heat flux removal
    - Application to possible EAST gas cooled limiter and DEMO relevant FW with
  - Thermomechanics for FW/Divertor components
    - Analysis of post PRD design

Outline

- PFC Heat and Mass Transfer Simulation
  - Tritium retention and permeation in FW/Divertor
  - Helium cooling for high heat flux removal
  - Thermomechanics for FW/Divertor components
- Synergistic Blanket Research
  - Liquid metal MHD, heat and tritium transport
    - E.g. High temperature liquid metal loop for channel flow
  - Ceramic breeder and Be thermomechanics and tritium transport

High Temperature LM loop and experiments

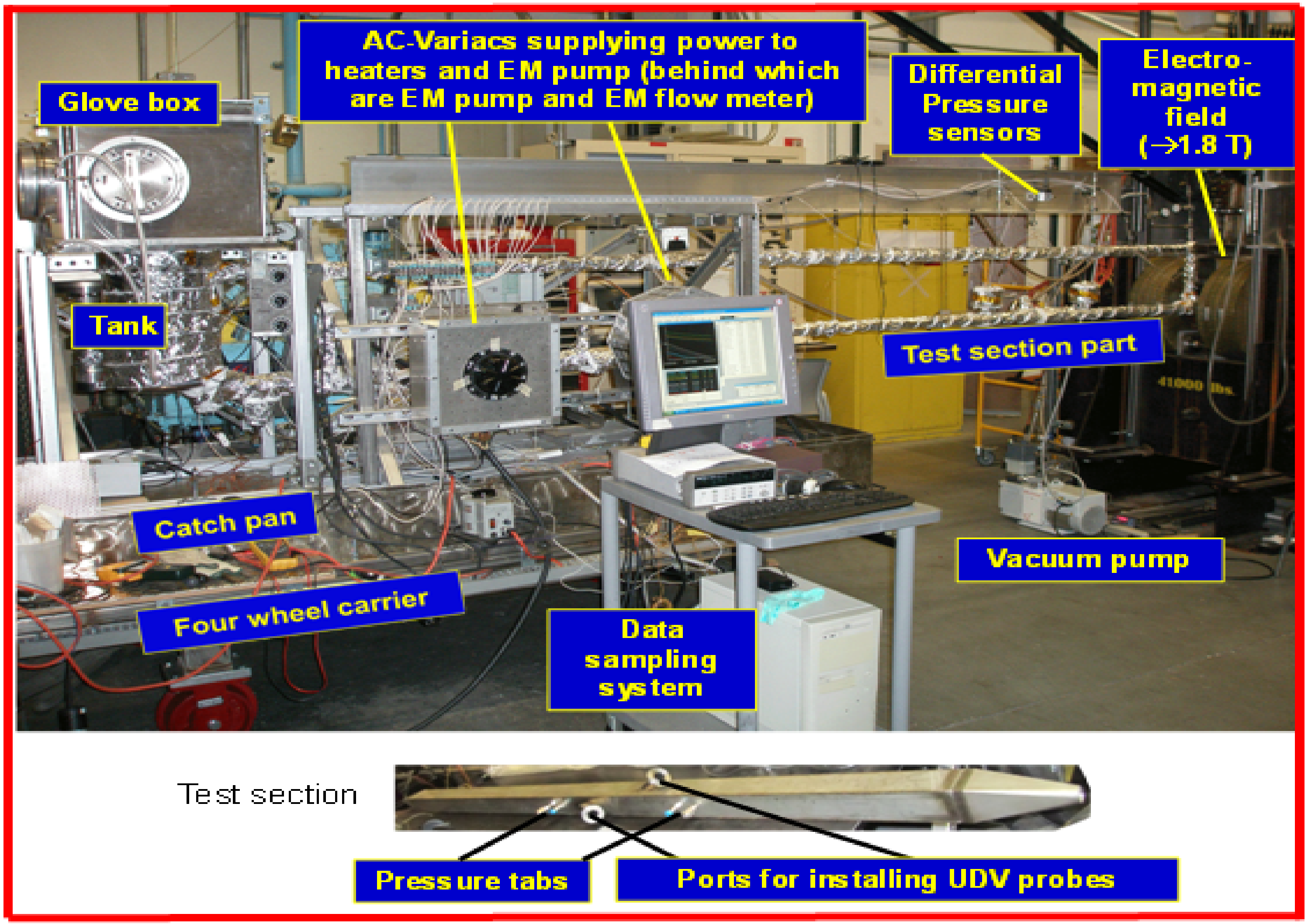

Photograph of a newly-constructed (2011) MHD PbLi loop at UCLA

PbLi, 400C
EM cond. Pump

1st experiment:
flow channel insert MHD performance

PbLi measurement and technology development

LM-MHD simulation development and coupling to heat, tritium and corrosion transport

Mobilization of liquid layer by body forces

- Experiments on simple systems
  - JxB force, vertical on wetted layer
  - JxB force, horizontal on wetted layer
  - Centrifugal force, horizontal wetted foams and wetted layers
- Simulations of Rayleigh-Taylor instabilities with strong body forces and plasma wind

JxB force, vertical on wetted layer

Ga-In-Sn Properties

ρ = 6330 kg/m3

$\sigma = 3 \times 10^{6}\ \Omega^{-1}\ m^{-1}$

$\nu = 4 \times 10^{-7}\ m^{2}/s$

χ = 0.55 N/m

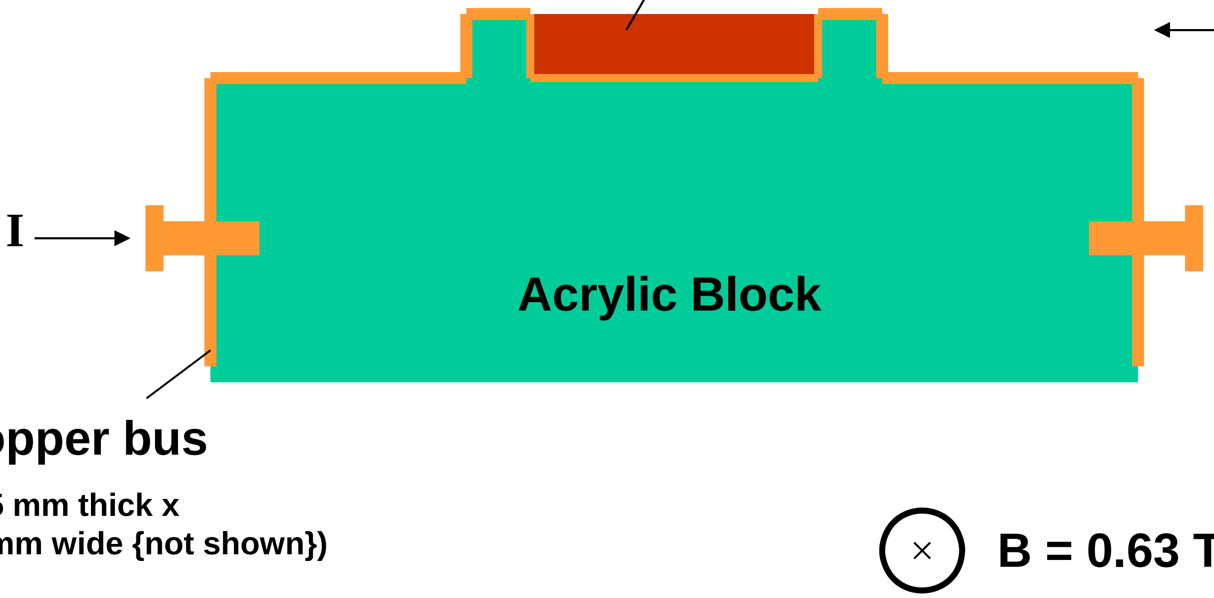

Ga-In-Sn Pool

11 mm long x 2 mm deep x
12 mm wide {not shown}

View perspective

I

Gnd

Acrylic Block

Copper bus

0.25 mm thick x
12 mm wide {not shown})

B = 0.63 T

Vertical “surface normal” forces can remove excess liquid metal from a wetted surface

- Shallow pool of liquid metal, and/or
- Liquid above trenches or capillary restraint

	20 A	50 A	80 A
J_0, kA/cm2	2.5	6.3	10.1
Mag Force / Gravity	2.6 (0.2)	6.4 (0.5)	10.2 (0.8)
Magnetic / ST Force	1.7 (1.8)	4.3 (4.4)	6.8 (6.9)
Qualitative Result	Some deformation	Very large deformation	Complete detachment
Rise Time, ms	20	30	35

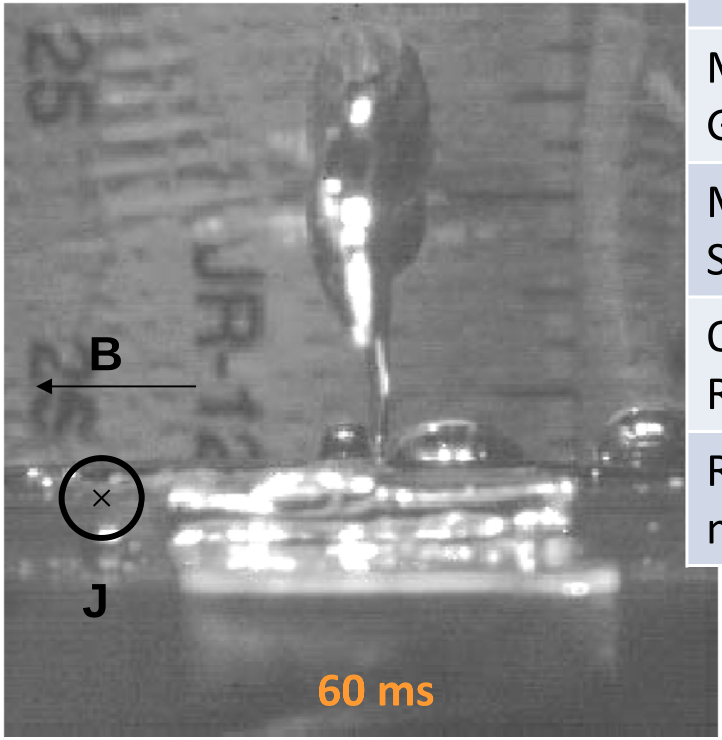

Keeping liquid layer below solid surface exposes edges

Horizontal centrifugal force to remove wetted liquid layers

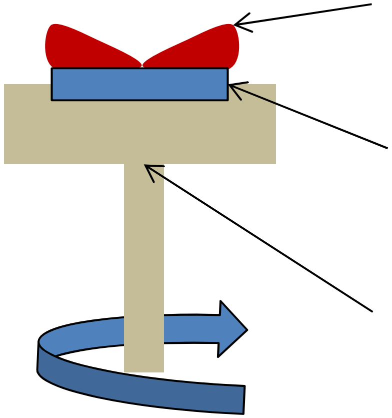

Liquid metal pushed off by centrifugal force

Sample, foams or dendritic surfaces

Rotating device

Excess surface layers removed, but LM in pores not removed

- 100 ppi W foam (Ultramet)
- Wetted Ga-In-Sn
- Max Spin/ STF ratio ~0.4


Before, extra loading of LM ~ 1mm

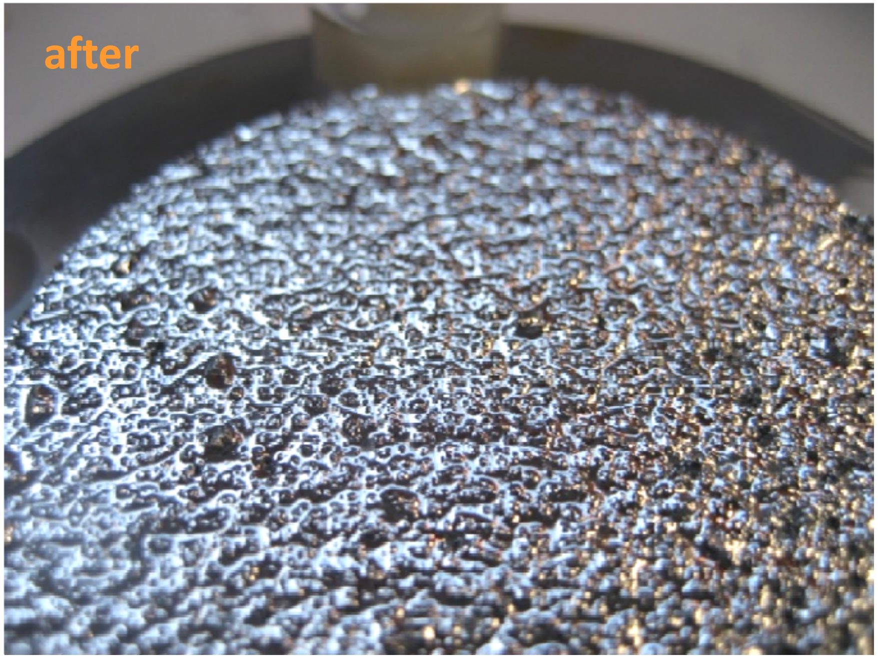
after

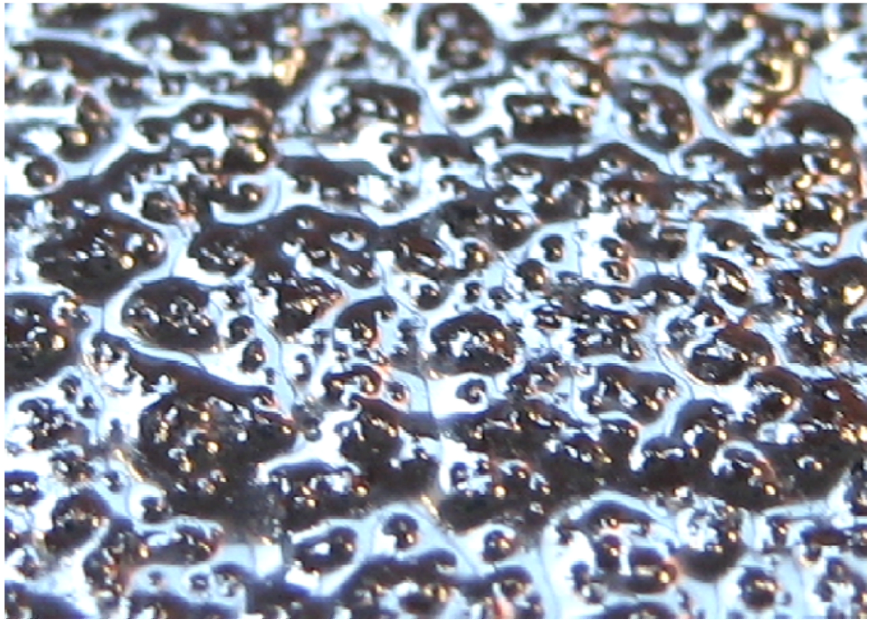

2D TE-MHD Test Case
Long thin grooves filled with Li

- 400 μm wide x 1 cm deep Li channel made from 100 μm thick Molybdenum
- 1 MW/m2 uniform surface heat flux
- Lithium flow driven by TEMHD currents generated from surface heat flux
- Coupled fully developed TE-MHD flow and heat transfer calculated
- New "thin" conducting wall BC with TE terms used to simulate conducting wall

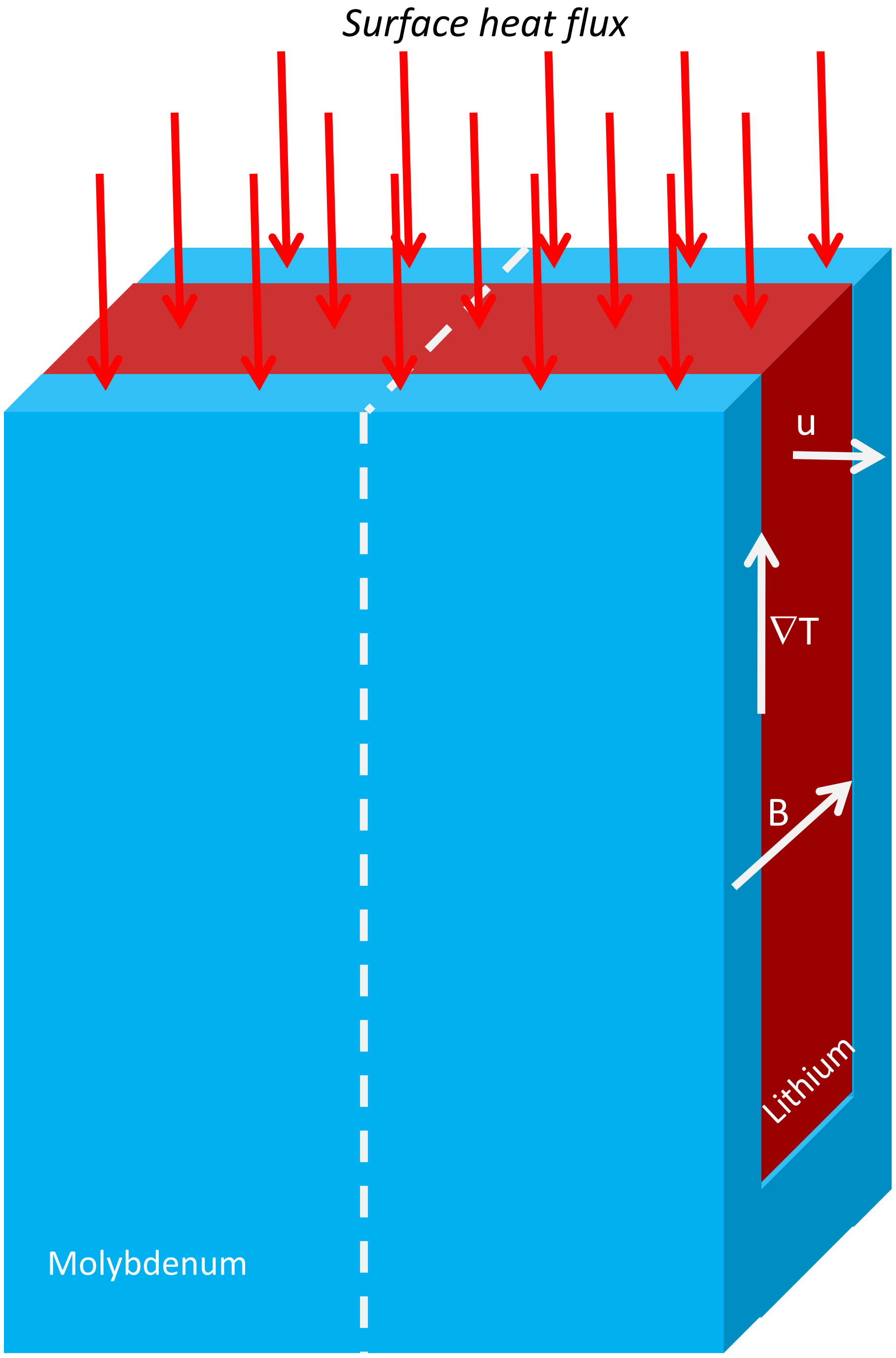

2D Velocity and Temperature Profile of TEMHD driven flow

- Peak surface velocity ~ 20 cm/s
- Surface temperature rise (from bulk to surface), ~ 40 K
- TE currents confined to Hartmann boundary layer

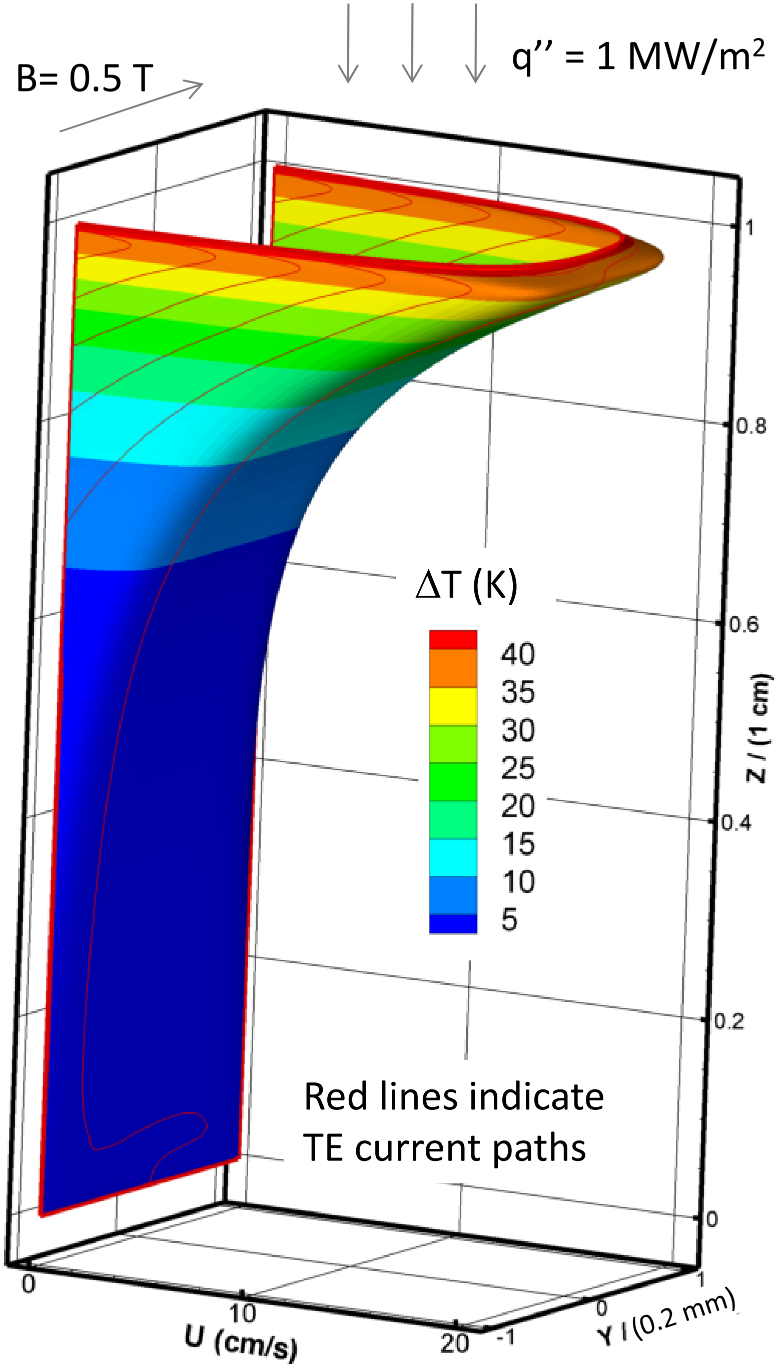

Red lines indicate TE current paths